Polarization evolution accompanying the very early sharp decline of GRB X-ray afterglows

Yi-Zhong Fan[1,2,3*], Dong Xu[4] and Da-Ming Wei[1,2,5]

[1]*Purple Mountain Observatory, Chinese Academy of Sciences, Nanjing 210008, China*
[2]*National Astronomical Observatories, Chinese Academy of Sciences, Beijing 100012, China*
[3]*Niels Bohr Institute, Neils Bohr International Academy, Blegdamsvej 17, DK-2100 Copenhagen, Denmark*
[4]*Dark Cosmology Centre, Niels Bohr Institute, University of Copenhagen, Juliane Maries Vej 30, 2100 Copenhagen, Denmark*
[5]*Joint Center for Particle Nuclear Physics and Cosmology of Purple Mountain Observatory - Nanjing University, Nanjing 210008, China.*

ABSTRACT
In the synchrotron radiation model, the polarization property depends on both the configuration of the magnetic field and the geometry of the visible emitting region. Some peculiar behaviors in the X-ray afterglows of *Swift* gamma-ray bursts (GRBs), such as energetic flares and the plateau followed by a sharp drop, might by highly linearly-polarized because the outflows powering these behaviors may be Poynting-flux dominated. Furthermore, the broken-down of the symmetry of the visible emitting region may be hiding in current X-ray data and will give rise to interesting polarization signatures. In this work we focus on the polarization accompanying the very early sharp decline of GRB X-ray afterglows. We show that strong polarization evolution is possible in both the high latitude emission model and the dying central engine model which are used to interpret this sharp X-ray decline. It is thus not easy to efficiently probe the physical origin of the very early X-ray sharp decline with future polarimetry. Strong polarization evolution is also possible in the decline phase of X-ray flares and in the shallow decline phase of X-ray light curves characterized by chromatic X-ray VS. Optical breaks. An *XRT*-like detector but with polarization capability on board a *Swift*-like satellite would be suitable to test our predictions.

Key words: Gamma Rays: bursts − polarization − GRBs: jets and outflows − radiation mechanisms: nonthermal

1 INTRODUCTION

The successful launch of the *Swift* satellite in Nov 2004 opened a new window to reveal what has been happening in the early afterglow phase of gamma-ray bursts (GRBs). As summarized in Zhang et al. (2006) and Nousek et al. (2006), in a canonical *Swift* GRB X-ray afterglow lightcurve some interesting features are emerging (detected in a good fraction of but not all bursts), including a very early sharp decline (phase-I), a shallow decline or even plateau, (phase-II), preceding the conventional or so-called "normal" decay phase (phase-III & -IV), and the energetic X-ray flares (phase-V). Various modifications of the standard GRB afterglow model have been put forward to explain the observations (see Mészáros 2006; Piran & Fan 2007; Zhang 2007 for recent reviews). Although the underlying physical processes are not very clear, it is widely suggested that the X-ray Phases I, II and V may be relevant to prolonged activities of the central engine while the simultaneous optical afterglow is dominated by GRB forward shock emission (Fan & Wei 2005; Zhang et al. 2006; Ghisellini et al. 2007; Panaitescu 2007). If so, the early time UV/optical and X-ray polarization behaviors should be independent and may be very different from each other. In some models, the outflows powering energetic flares and X-ray plateaus followed by a sharp drop are Poynting-flux dominated (e.g., Gao & Fan 2006; Giannios 2006; Troja et al. 2007), thus high-linear polarization of these synchrotron radiation photons is expected (Fan, Zhang & Proga 2005).

---

* E-mail: yzfan@pmo.ac.cn

Except the configuration of the magnetic field, the geometry of the emitting area can influence the polarization property of the synchrotron radiation as well. The broken-down of the symmetry of the visible emitting region may be hiding in the peculiar X-ray data and can give rise to interesting polarization signatures. Motivated by this idea, in section 2 we calculate the polarization property of Phase-I and show that strong evolution is likely. In section 3, we argue that similar phenomena are also expected in the decline phase of the X-ray flares and possibly in the late time part of Phase-II, especially those associated with a chromatic break in optical band. We also discuss the detection prospect there. In section 4, we summarize our work with some discussions.

2 THE POLARIZATION EVOLUTION ACCOMPANYING PHASE-I

For phase-I, two leading interpretations are: (i) these X-ray photons are actually the high latitude emission of a main internal shock pulse (Fenimore et al. 1996; Kumar & Panaitescu 2000; Zhang et al. 2006) while the central engine has died; and (ii) these X-ray photons are powered by the weaker and weaker activity of the central engine, i.e., the sharp X-ray decline traces the activity of the dying central engine (Fan & Wei 2005; Piran & Fan 2007)[1]. The interpretation (i) has been widely accepted because some X-ray declines can be adjusted as $\propto (t - t_0)^{-(2+\beta_X)}$ predicted by the high latitude emission model (Liang et al. 2006; Yamazaki et al. 2006; Zhang, Liang & Zhang 2007a), where β_X is the X-ray spectral index, and t_0 is a free parameter parameterizing the beginning of a certain internal shock pulse [2]. Such a test, however, is not conclusive. As shown in Sakamoto et al. (2007), for the very sharp X-ray decline, the data itself can not well constrain the function form $(t - t_0)^{-k}$. In many events, k can be taken as a constant (for example, $k \sim 2$) and thus is not relevant to β_X. Additionally, it is not easy to see why the GRB central engine turns off abruptly while the numerical simulation actually shows the contrast (MacFadyen et al. 2001; Zhang, Woosley & Heger 2007b). Interpretation (i) also fails to interpret some slowly decaying phase-I as in GRB 060614 (Butler & Kocevski 2007; Zhang *et al.* 2007a; Xu et al. 2008). As for interpretation (ii), there has been no strict observational test so far though it seems possible for any energetic burst phenomenon.

We take into account both models in our calculation and examine the possibility to distinguish between these two models with future X-ray polarimetry.

2.1 High latitude emission model

If interpretation (i) is correct, i.e., the sharp X-ray decline is due to the high latitude emission of a main internal shock pulse, there would be very interesting polarization signals. As is known, GRB outflow is likely to be jetted. In this work we only consider the uniform jet model. Following Ghisellini & Lazzati (1999), we assume that the half-opening angle of the ejecta is θ_j, and that the line of sight (L.o.S.) makes an angle θ_v with respect to the jet's central axis (C.A., see Fig.1a for illustration). The probability of observing the ejecta along its C.A. is vanishingly small since it corresponds a very small solid angle. For typical bright GRBs, the L.o.S. is likely to be within the cone, i.e., $\theta_v < \theta_j$. At early time, the high latitude emission is from zones around the L.o.S. satisfying $\theta \leqslant \theta_j - \theta_v$, so the net polarization of the detected photons vanishes because of the symmetry; but at later time, the high latitude emission is from $\theta > \theta_j - \theta_v$, the symmetry is broken and the observed net polarization is not zero any longer.

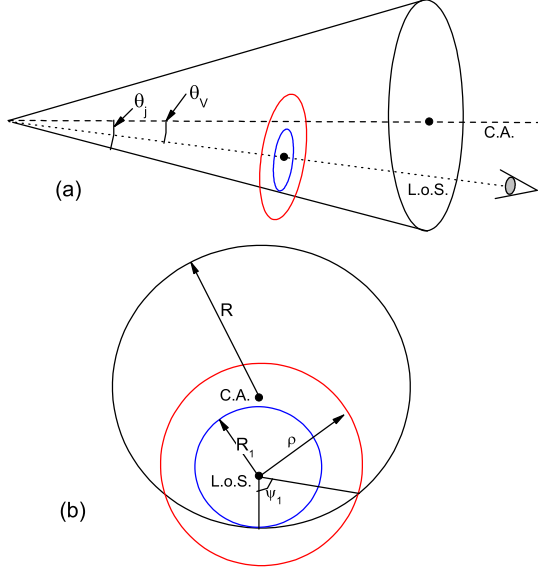In this model, the photons arrived at t were emitted from

$$\theta \approx (2ct/R_0)^{1/2}, \tag{1}$$

where $R_0 \sim R_{\rm prompt}$ is the radius of the main internal shock pulse and c is the speed of light. Below we adopt the simplified calculation of Ghisellini & Lazzati (1999). The notations used in Fig.1b are related to R_0, θ_j and θ_v as $R \approx R_0 \sin\theta_j$ and $R_1 \approx R_0 \sin(\theta_j - \theta_v)$. When $\rho > R_1$, the ring is not a complete circle. The missing parts are in $(0, \psi_1)$ and $(2\pi - \psi_1, 2\pi)$ as shown in Fig.1. Approximately, we have (Ghisellini & Lazzati 1999)

$$\psi_1 \approx \begin{cases} \frac{\pi}{2} - \arcsin\left[\frac{2R_1 R - R_1^2 - \rho^2}{2\rho(R - R_1)}\right], & \text{for } \rho > R_1; \\ 0, & \text{for } \rho < R_1, \end{cases} \tag{2}$$

---

[1] These two interpretations can be also applied to the sharp decline of the X-ray flares.

[2] In this interpretation, the duration of the main prompt emission pulse should be in order of the timescale of whole burst otherwise the total high latitude emission of those early pulses decay too fast to account for the observation (see Fig.2 of Fan & Wei 2005 for illustration). This is somewhat unusual in the standard internal shock model, in which the typical variability timescale is just in order of milliseconds. A possible solution of this puzzle is to assume that the prompt $\gamma-$ray emission are powered by some magnetic energy dissipation processes at a distance $R_{\rm prompt} \sim 10^{15} - 10^{16}$ cm to the central engine, so the emission duration is governed by the angular timescale $\sim R_{\rm prompt}/(2\Gamma^2 c) \sim 6(R_{\rm prompt}/10^{15}$ cm$)(\Gamma/50)^{-2}$ sec, where Γ is the bulk Lorentz factor of the outflow.

Figure 1. (a) The high latitude emission model for the X-ray decline. The larger the angle with respect to the line of sight (L.o.S), the latter the emission arrives at us because of the geometry effect. (b) Sketch of the geometrical set-up used to compute the polarization signal (see also Ghisellini & Lazzati 1999).

where $\rho \approx R_0 \sin\theta$.

In principle, the GRB outflow could be either baryon-rich or Poynting-flux dominated. For the former the magnetic field is generated in the shock front and is likely to be random. For the latter the magnetic field is coherent in a large scale. The resulting polarization light curves are expected to be different in these two cases, as shown below.

Random magnetic field. The net polarization of the emission from $\rho - \rho + d\rho$ can be approximated by (See the Appendix for the derivation)

$$\Pi(\rho) \approx \Pi_0 \frac{(2\zeta^2 - 1)\sin^2\alpha}{2\zeta^2 \sin^2\alpha + (1 + \cos^2\alpha)} \frac{|\sin(2\psi_1)|}{2\pi - 2\psi_1}, \tag{3}$$

where Π_0 is the maximum polarization at one point, α is the viewing angle with respect to the fluid velocity in the outflow comoving frame (see Figure A1 for illustration), which is governed by $\cos\alpha = (\cos\theta - \beta)/(1 - \beta\cos\theta)$, and the parameter $\zeta^2 = <B_\parallel^2> / <B_\perp^2>$ denotes the level of anisotropy of the magnetic field distribution, where $B_\perp$ and $B_\parallel$ are magnetic field perpendicular and parallel to the normal of the shock plane. $\beta = (1 - 1/\Gamma^2)^{1/2}$ is the velocity of the GRB ejecta in units of c.

We note that in eq.(3) $\Pi(\rho) \propto \sin^2\alpha/(1 + \cos^2\alpha)$ if $\zeta^2 \sim 0$. For $\Gamma(\theta_j - \theta_v) \gg 1$, we have $\Pi(\rho) \propto 2\Gamma^2(\theta_j - \theta_v)^2/[1 + \Gamma^4(\theta_j - \theta_v)^4] \ll 1$. The resulting net polarization can thus be neglected. But for $2\zeta^2 \sin^2\alpha \gg 1 + \cos^2\alpha$, the second term in the right side of eq.(3) is $\to 1$. Significant net polarization is possible.

As $\theta > (\theta_j - \theta_v)$, the observers just detected $\sim (\pi - \psi_1)/\pi$ part of the circle, the X-ray flux will decline more steeply than $t^{-(2+\beta_X)}$ and is governed by

$$F_X(t) \propto \frac{\pi - \psi_1(t)}{\pi} t^{-(2+\beta_X)}. \tag{4}$$

We plot in Fig.2 the sharp X-ray decline and the corresponding polarization light curves. When the emission is from a circle ring, the net polarization is zero because of the symmetry. As θ is getting larger and just part of the ring is visible, the observed polarization degree is not zero any longer until $\rho^2 \to 2R_1 R - R_1^2$ (i.e., $\psi_1 \to \pi/2$). At the point of $\psi_1 = \pi/2$, the net polarization becomes zero again according to equation (3), because the polarization direction abruptly changes by $\pi/2$. After this point, the polarization increases again. But the flux may be too weak to have a significant polarization measurement.
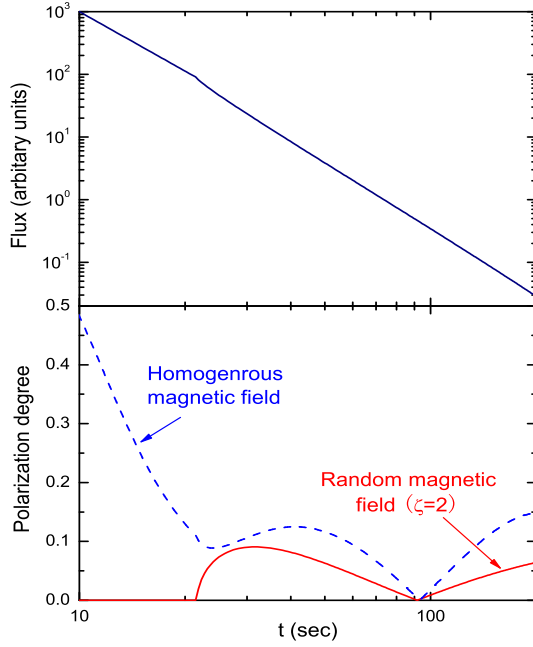
Homogenous magnetic field. In this case, the instantaneous stokes parameters (note that $V = 0$ as the polarization is linear) and the polarization degree are given by (Granot & Königl 2003):

$$\frac{\left\{ \begin{array}{c} Q \\ U \end{array} \right\}}{I} = \Pi_0 \frac{\int_{\psi_1}^{2\pi - \psi_1} [(\frac{1-y}{1+y})^2 \cos^2\phi + \sin^2\phi]^{\epsilon/2} \left\{ \begin{array}{c} \cos(2\theta_p) \\ \sin(2\theta_p) \end{array} \right\} d\phi}{\int_{\psi_1}^{2\pi - \psi_1} [(\frac{1-y}{1+y})^2 \cos^2\phi + \sin^2\phi]^{\epsilon/2} d\phi}, \tag{5}$$

and

$$\Pi = \frac{\sqrt{U^2 + Q^2}}{I}, \tag{6}$$

where $\theta_p = \phi + \arctan(\frac{1-y}{1+y}\cot\phi)$, $y = \Gamma^2\theta^2$ and $\epsilon = (1 + \beta_X)/2$ (Granot & Königl 2003). Again the polarization light curve

4

Figure 2. The sharp X-ray decline (upper panel) and the corresponding polarization light curves (lower panel) after a time-shift correction, in the case of the high latitude emission model. For this figure we assumed $\Pi_0 = 60\%$, $\Gamma = 50$, $\theta_j = 0.1$, $\theta_v = 0.07$, $R_0 = 10^{15}$ cm and $\beta_X = 1.15$.
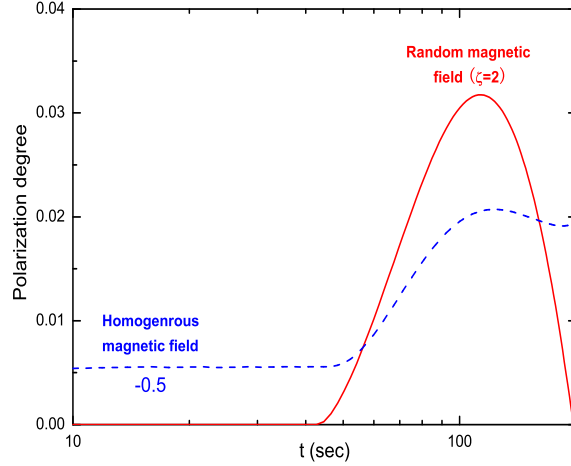
has been plotted in Fig.2, which is similar to that of the random magnetic field case except an initial high polarization degree. This strongly suggests that the late time non-zero polarization is mainly contributed by the geometry effect, as in the case of a random magnetic field. If the symmetry has not been broken down, the late time net polarization for an ordered magnetized outflow disappears, as already found in Nakar, Piran & Waxman (2003).

2.2 Dying central engine model

Generally, in the dying central engine model there are two possibilities. (1) If the outflow powering the fast decaying X-ray tail emission always has a Lorentz factor $\Gamma > 1/(\theta_j - \theta_v)$, no strong polarization evolution is expected unless the physical composition of the outflow has changed a lot (e.g., from byron dominated to Poynting-flux dominated). We thus may be able to distinguish between the high latitude emission model and the dying central engine model with the future X-ray polarimetry. (2) The bulk Lorentz factor of the outflow drops so quickly as to satisfy $\Gamma < 1/(\theta_j - \theta_v)$ in a short period. When $\Gamma < 1/(\theta_j - \theta_v)$, the symmetry of the visible emitting area is broken and interesting polarization signature begins to exist. Since there is little information about the evolution of Γ with t, we here simply assume $\Gamma \approx 150(t/10)^{-1}$ for $10 < t < 200$ sec and θ_j and θ_v are constant. Again, we calculate the polarization evolution in the cases of *random magnetic field* and *Homogenous magnetic field*. But now the calculation should be due to the emission area within $\theta \leqslant 1/\Gamma$, rather than from a ring at θ in the high latitude emission model. Therefore, we calculate the quantities of (Q, U, I) along the radius ρ and integrate them over ρ. Such calculations have been carried out by Ghisellini & Lazzati (1999) and Granot & Königl (2003), respectively. Our numerical results are presented in Figure 3. One can see that polarization evolution is evident and shares some similarity with that in Fig.2, particularly in the case of *random magnetic filed*, though the polarization degree of high latitude emission model is larger than that of the dying central engine model. This is reasonable since in the former case the emission is from the ring while in the latter case the emission is from $\theta \leqslant 1/\Gamma$. In the case of *homogenous magnetic filed*, the evolution is small because of the significant polarization background (the degree is ~ 0.5) caused by the ordered magnetic field from the central source.

3 PROSPECT OF DETECTING THE X-RAY POLARIZATION

Our calculations in Section 2 are actually applicable to more phases in the GRB X-ray afterglow light curve. One is the decline phase of X-ray flares (in Phase-V), which is also attributed to the high latitude emission model or the dying (re-)activity of the central engine. The other is the late phase of the X-ray flattening (in Phase-II). Recently Ghisellini et al. (2007) interpreted Phase-II, particularly those show chromatic breaks in X-ray and optical bands, as the prolonged emission of the central engine. The X-ray flattening ceases to exist when the bulk Lorentz factor of the outflow is so small that one sees the edge of the

Figure 3. The polarization light curves in the case of dying central engine model. The physical parameters are the same as that of Fig.2 except we assume $\Gamma = 150(t/10)^{-1}$ for $10 < t < 200$ sec. Please note that the dashed line is not the real polarization degree unless a factor 0.5 has been added.

outflow. If these interpretations are correct, strong polarization evolution should be present at the end of Phase-II and in the decline of Phase-V.

Measuring polarization is of growing interest in high energy astronomy. New technologies are being invented, and several polarimeter projects are under construction. In the X-ray band, the ongoing projects include XPE (Elsner et al. 1997), PLEXAS (Marshell et al. 1998), POLAR (Produit et al. 2005), XPOL (Costa et al. 2006), POET (Polarimeters for Energetic Transients, see McConnel et al. 2007), and so on. For example, the planned POET includes two instruments: GRAPE (Gamma-Ray Polarimeter Experiment) and LEP (Low Energy Polarimeter, working in soft X-ray band). So it may be suitable to detect the polarization signatures predicted in the early X-ray afterglow of GRBs. An important issue is whether any of these detectors could perform a prompt slew to the GRBs localized by the $\gamma-$ray monitor. An ideal instrument would be an XRT-like detector with polarization capability on board a *Swift*-like GRB mission.

4 SUMMARY & DISCUSSION

Many surprises in GRB afterglows, mainly in the X-ray band, have been brought since the successful launch of *Swift* in 2004. Though not clearly understood yet, the (re-)activity of GRB central engine is likely to play an important role on producing afterglows, as speculated by Katz, Piran & Sari (1998). The different temporal behaviors in the UV/optical and X-ray afterglow favor that the peculiar X-ray emission traces the prolonged activity of the central engine while the optical afterglow is dominated by the forward shock emission (Fan & Wei 2005; Ghisellini et al. 2007). If true, the polarization behaviors of the early X-ray and optical afterglow may be independent and different. At such an early time, the linear polarization of the optical forward shock emission is expected to be very small (Ghisellini & Lazzati 1999) unless the interstellar medium is magnetized (Granot & Konigel 2003), because the Lorentz factor of the outflow is so large that the visible emitting region is well within the cone of the ejecta and is thus symmetric. But in the X-ray band, interesting polarization signatures may be present. For example, Fan et al. (2005) argued that some X-ray flares might have a high linear polarization because these new outflows are likely to be Poynting-flux dominated. Such an argument is also applicable to the X-ray plateau followed by a sharp drop as detected in GRB 070110.

In this work, we focus on the polarization properties of the very early sharp decline of X-ray afterglows (Phase-I). In the high latitude emission model, the later the emission, the larger the angular θ (see Figure 1 for details). So at late time, the symmetry of the emitting ring is broken when part of the emitting ring is out of the cone of the ejecta. Strong polarization evolution thus emerges (see Section 2.1). For comparison, results from the dying central engine model are a bit more complicated. If the outflow powering the fast decaying X-ray tail emission always has a Lorentz factor $\Gamma > 1/(\theta_j - \theta_v)$, no strong polarization evolution is expected unless the physical composition of the outflow changed significantly. However, if the Lorentz factor drops rapidly to satisfy $\Gamma < 1/(\theta_j - \theta_v)$, then polarization evolution is evident. In this scenario, if the magnetic field involved is shock-generated and is thus random, then strong polarization evolution is expected; while if the magnetic field involved is brought from the central engine and is thus large-scale ordered, then weak polarization evolution is expected due to the significant polarization background (the degree is ~ 0.5). One of our goals to calculate the polarization

of Phase-I is to see whether it's possible, via X-ray polarimetry, to distinguish between the high latitude emission model and the dying central engine model. This goal is not easy to fulfill in view of the above comparison. However, our calculation does support that strong polarization evolution is likely to accompany Phase-I, the decline phase of X-ray flares (Phase-V) and possibly the late part of Phase-II. Fruitful novel features are expected to appear in GRB X-ray afterglow polarimetry, though detection of them is beyond the capability of current monitors. We have witnessed the breakthrough made by *Swift* XRT and we are likely to experience it once more in the coming X-ray polarimetry era. One byproduct of the future X-ray polarimetry is to probe the cosmological birefringence effect that arises in some quantum gravity models (Fan, Wei & Xu 2007 and the references therein).
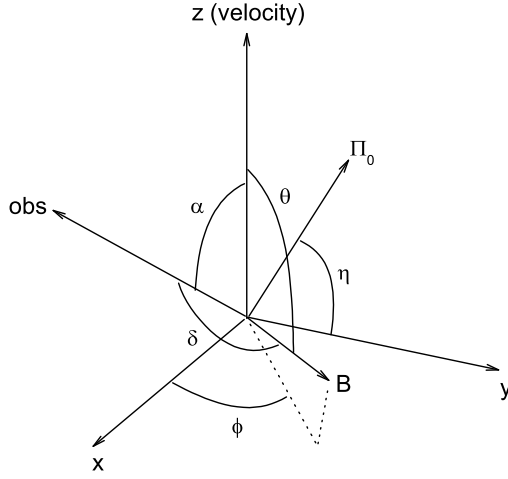
Finally we'd like to point out that the optical flares in a few bursts (e.g., Böer et al. 2006) may also have a central engine origin (Wei, Yan & Fan 2006). Interesting polarization signatures are also expected.

REFERENCES

Boër, M., Atteia, J. L., Damerdji, Y., Gendre, B., Klotz, A., & Stratta, G. 2006, ApJ, 638, L71
Butler N. R., Kocevski D., 2007, ApJ, 663, 407
Costa E., et al., 2006, Proc. 39th ESLAB Symposium, SP-588, 141, edited by F. Favata and A. Gimenez.
Elsner R. F. et al., 1997, 190th AAS Meeting, #09.11; Bulletin of the American Astronomical Society, Vol. 29, 790
Fan Y. Z., Wei D. M., 2005, MNRAS, 364, L42
Fan Y. Z., Wei D. M., Xu D., 2007, MNRAS, 376, 1857
Fan Y. Z., Zhang B., Proga D., 2005, ApJ, 635, L129
Fenimore E. E., Madras C. D., Nayakshin S., 1996, ApJ, 473, 998
Gao W. H., Fan Y. Z., 2006, Chin. J. Astron. Astrophys, 6, 513
Ghisellini G., Ghirlanda G., Nava L., Firmani C., 2007, ApJ, 658, L75
Ghisellini G., Lazzati D., 1999, MNRAS, 309, L7
Giannios D., 2006, A&A, 455, L5
Granot J., Konigel A., 2003, 594, L83
Gruzinov A., 1999, ApJ, 525, L29
Katz J. I., Piran T., Sari R., 1998, Phys. Rev. Lett., 80, 1580
Kumar P., Panaitescu A., 2000, ApJ, 541, L51
Liang E. W. *et al.*, 2006, ApJ, 646, 351
MacFadyen A. I., Woosley S. E., Heger A., 2001, ApJ, 550, 410
McConnel M. et al. 2007, Poster at the Santa Fe meeting
Marshall, H. L. et al. 1998, 192nd AAS Meeting, #35.04; Bulletin of the American Astronomical Society, Vol. 30, 860
Mészáros P., 2006, Rep. Prog. Phys, 69, 2259
Nakar E., Piran T., Waxman E., 2003, JCAP, 0310, 005
Nousek J. A., et al., 2006, ApJ, 642, 389
Panaitescu A., 2007, MNRAS, in press (arXiv:0708.1509)
Piran T., Fan Y. Z., 2007, Phil. Trans. R. Soc. A., 365, 1151
Produit, N., et al. 2005, Nucl. Instrum. Methods. Phys. Res. Sec. A, 550, 616
Sakamoto T. et al., 2007, ApJ, 669, 1115
Sari R., 1999, ApJ, 524, L43
Troja E. *et al.*, 2007, ApJ, 665, 599
Wei D. M., Yan T., Fan Y. Z., 2006, ApJ, 636, L69
Xu D., et al., 2008, ApJ, to be submitted
Yamazaki R., Toma K., Ioka K., Nakamura T., 2006, MNRAS, 369, 311
Zhang B., 2007, ChJAA, 7, 1
Zhang B., Fan Y. Z., Dyks J., Kobayashi S., Mészáros P., Burrows D. N., Nousek J. A., Gehrels N. 2006, ApJ, 642, 354
Zhang B. B., Liang E. W., Zhang B., 2007, ApJ, 666, 1002
Zhang W. Q., Woosley S. E., Heger A., 2007, ApJ, in press (astro-ph/0701083)

Figure A1. The coordinate system to optimize the derivation (see also Sari 1999).

APPENDIX A: DERIVATION OF EQUATION (3) IN THIS WORK

Obviously, first we need to establish a suitable coordinate system to optimize the derivation. As stated in Sari (1999), at any point in the shock front there is a preferred direction, the radial direction, in which the fluid moves. We call this the parallel direction and choose the z-direction of the fluid local frame coordinate system to be in that direction. The two perpendicular directions (x, y) are assumed equivalent, i.e., the system is isotropic in the plane perpendicular to the direction of motion. We chose the x-direction to be in the plane that contains the z-direction and the direction towards the observer $\hat{n}$, as shown in Figure A1. Suppose now that the magnetic field has spherical coordinates (θ, φ) in that frame. A quite general description of the distribution of the magnetic field in such anisotropic system would be to allow different values of the magnetic field as function of the inclination from the preferred direction $B = B(\theta)$ as well as a probability function for the magnetic field to be in each given inclination $f(\theta)$.

The relevant component of the magnetic field is that perpendicular to the observer i.e. $B \sin(\delta)$, where δ is the angle between the direction of the magnetic field and the observer. This will produce polarization Π_0 in the direction perpendicular both to the observer and to the magnetic field i.e. in the direction $\hat{n} \times \hat{B}$. However, this polarization should be averaged due to contributions from magnetic fields oriented differently. On the other hand, because light is a kind of transverse wave, its polarization should be perpendicular to its propagation. Therefore, we project the polarization to $\hat{y}$ (i.e., the component Q) and $\hat{n} \times \hat{y}$ (i.e., the component U), respectively.

Assuming that the emission is proportional to a certain power of the magnetic field, $\propto B^\epsilon$, the total polarization from a point-like region is then[3]

$$Q = \Pi_0 \int \cos(2\eta)[B(\theta) \sin \delta]^\epsilon f(\theta) \sin \theta d\phi d\theta, \tag{A1}$$

and

$$U = \Pi_0 \int \sin(2\eta)[B(\theta) \sin \delta]^\epsilon f(\theta) \sin \theta d\phi d\theta, \tag{A2}$$

and

$$I = \Pi_0 \int [B(\theta) \sin \delta]^\epsilon f(\theta) \sin \theta d\phi d\theta. \tag{A3}$$

Since $\hat{n} = (\sin \alpha, \ 0, \ \cos \alpha)$ and $\hat{B} = (\sin \theta \cos \phi, \ \sin \theta \sin \phi, \ \cos \theta)$, we have

$$\hat{\Pi} = \hat{n} \times \hat{B} = (-\cos \alpha \sin \theta \sin \phi, \ \cos \alpha \sin \theta \cos \phi - \sin \alpha \cos \theta, \ \sin \alpha \sin \theta \sin \phi).$$

With $\hat{y} = (0, \ 1, \ 0)$, we obtain

$$\cos \eta = \frac{\hat{\Pi} \cdot \hat{y}}{|\hat{\Pi}|} = \frac{\cos \alpha \sin \theta \cos \phi - \sin \alpha \cos \theta}{[\sin^2 \theta \sin^2 \phi + (\cos \alpha \sin \theta \cos \phi - \sin \alpha \cos \theta)^2]^{1/2}},$$

---

[3] where we have taken into account the fact that $\hat{y}$, $\hat{n} \times \hat{y}$ and $\hat{\Pi} = \hat{n} \times \hat{B}$ are all on the same plane which is perpendicular to $\hat{n}$.

and

$$\sin \eta = \frac{\sin \theta \sin \phi}{[\sin^2 \theta \sin^2 \phi + (\cos \alpha \sin \theta \cos \phi - \sin \alpha \cos \theta)^2]^{1/2}}.$$

From the forms of $\cos \eta$ and $\sin \eta$, we have

$$\cos(2\eta) = 2\cos^2 \eta - 1 = \frac{(\cos \alpha \sin \theta \cos \phi - \sin \alpha \cos \theta)^2 - \sin^2 \theta \sin^2 \phi}{\sin^2 \theta \sin^2 \phi + (\cos \alpha \sin \theta \cos \phi - \sin \alpha \cos \theta)^2}, \tag{A4}$$

and

$$\sin(2\eta) = 2\sin \eta \cos \eta = \frac{2\sin \theta \sin \phi(\cos \alpha \sin \theta \cos \phi - \sin \alpha \cos \theta)}{\sin^2 \theta \sin^2 \phi + (\cos \alpha \sin \theta \cos \phi - \sin \alpha \cos \theta)^2}. \tag{A5}$$

Now substitute equation (A5) into equation (A2), we get

$$
\begin{aligned}
U &= \Pi_0 \int \sin(2\eta)[B(\theta)\sin \delta]^\epsilon f(\theta) \sin \theta d\phi d\theta \\
&\propto \int \sin^2 \theta \sin \phi(\cos \alpha \sin \theta \cos \phi - \sin \alpha \cos \theta)|\hat{\Pi}|^{\epsilon-2} f(\theta) d\theta d\phi \\
&\propto \int_0^\pi \sin^2 \theta f(\theta) d\theta \int_0^{2\pi} \mathcal{F}(\phi, \alpha, \theta) d\phi.
\end{aligned}
\tag{A6}
$$

where $\mathcal{F}(\phi, \alpha, \theta) \equiv \frac{\sin \phi(\cos \alpha \sin \theta \cos \phi - \sin \alpha \cos \theta)}{[\sin^2 \theta \sin^2 \phi + (\cos \alpha \sin \theta \cos \phi - \sin \alpha \cos \theta)^2]^{(2-\epsilon)/2}}$, and we have taken $\sin \delta = |\hat{n} \times \hat{B}| = |\hat{\Pi}|$.

To calculate the integration for $\mathcal{F}(\phi, \alpha, \theta)$, we consider

$$\int_0^{2\pi} \mathcal{F}(\phi, \alpha, \theta) d\phi = [\int_0^{\pi/2} + \int_{\pi/2}^\pi + \int_\pi^{3\pi/2} + \int_{3\pi/2}^{2\pi}]\mathcal{F}(\phi, \alpha, \theta) d\phi. \tag{A7}$$

In regions of $\phi \in (0, \pi/2)$ and $\phi \in (3\pi/2, 2\pi)$, $\sin \phi$ changes the sign but $\cos \phi$ does not. So in the above integral the contribution from the angle ϕ has been cancelled out by that from $2\pi - \phi$. Similar results hold for the contribution of regions of $\phi \in (\pi/2, \pi)$ and $\phi \in (\pi, 3\pi/2)$. It is then straightforward to get

$$U \propto \int_0^{2\pi} \mathcal{F}(\phi, \alpha, \theta) d\phi = [(\int_0^{\pi/2} + \int_{3\pi/2}^{2\pi}) + (\int_{\pi/2}^\pi + \int_\pi^{3\pi/2})]\mathcal{F}(\phi, \alpha, \theta) d\phi = 0. \tag{A8}$$

We thus have proved that because of the isotropy of the magnetic field in the (x, y) direction, the polarization of radiation emitted from a point-like region (after averaging on magnetic field orientation) must be in the direction perpendicular to the z-axis and to the observer, i.e., in the $\hat{y}$ direction.

In the case of $\epsilon = 2$, both Q and I can be analytically integrated. With the relations $\int_0^{2\pi} \sin^2 \phi d\phi = \int_0^{2\pi} \cos^2 \phi d\phi = \pi$, we have

$$
\begin{aligned}
Q &\propto \int_0^\pi f(\theta) \sin \theta d\theta \int_0^{2\pi} B^2[(\cos \alpha \sin \theta \cos \phi - \sin \alpha \cos \theta)^2 - \sin^2 \theta \sin^2 \phi] d\phi \\
&= \pi \sin^2 \alpha \int_0^\pi B^2 f(\theta) \sin \theta [2\cos^2 \theta - \sin^2 \theta] d\theta,
\end{aligned}
\tag{A9}
$$

Note that $< B_\parallel^2 >= \int_0^\pi B^2 f(\theta) \sin \theta \cos^2 \theta d\theta$ and $< B_\perp^2 >= \int_0^\pi B^2 f(\theta) \sin^3 \theta d\theta$, we have

$$Q \propto 2\pi \sin^2 \alpha(< B_\parallel^2 > - \frac{< B_\perp^2 >}{2}).$$

Similarly,

$$I = \int_0^\pi f(\theta) \sin^2 \theta B^2 |\hat{\Pi}|^2 d\theta = 2\pi(\sin^2 \alpha < B_\parallel^2 > +(1 + \cos^2 \alpha) < B_\perp^2 > /2).$$

Therefore, the net polarization is given by (see also Gruzinov 1999 and Sari 1999)

$$P_{\text{point}} = \frac{Q}{I} = \Pi_0 \frac{\sin^2 \alpha(< B_\parallel^2 > - < B_\perp^2 > /2)}{\sin^2 \alpha < B_\parallel^2 > +(1 + \cos^2 \alpha) < B_\perp^2 > /2}. \tag{A10}$$

In the high latitude model for the X-ray sharp decline, the emission is from an angle α (or, equivalently ρ). As shown in Ghisellini & Lazzati (1999), it is convenient to write the polarization vector as a complex number $P = P_{\text{point}} e^{2i\theta_{\text{p}}}$ and integrate it between ψ_1 and $2\pi - \psi_1$. Here θ_{p} is the position angle of the linear polarization in the observer frame. The polarization of a generic ring is thus

$$\Pi(\rho) = \frac{\int_{\psi_1}^{2\pi-\psi_1} P_{\text{point}} I d\theta_{\text{p}}}{\int_{\psi_1}^{2\pi-\psi_1} I d\theta_{\text{p}}} = \Pi_0 \frac{(2\zeta^2 - 1)\sin^2\alpha}{2\zeta^2\sin^2\alpha + (1+\cos^2\alpha)} \frac{|\sin(2\psi_1)|}{2\pi - 2\psi_1}, \tag{A11}$$

where $\zeta^2 = <B_\parallel^2> / <B_\perp^2>$.

Till here, we thus have proved equation (3) in this work.